Flux crystal growth of lanthanide tungsten oxychlorides, $La_{8.64}W_6O_{30.45}Cl$, $Ce_{8.64}W_{5.74}O_{30}Cl$, and $Ln_{8.33}W_6O_{30}Cl$ (Ln = Pr, Nd): Structural stability in the presence of extreme cation and anion disorder

Darren Carone, Vladislav V. Klepov, Mark D. Smith, and Hans-Conrad zur Loye*

Department of Chemistry and Biochemistry, University of South Carolina, Columbia, SC 29208, USA

Abstract

A series of lanthanide tungsten oxychlorides with compositions of $La_{8.64}W_6O_{30.45}Cl$, $Ce_{8.64}W_{5.74}O_{30}Cl$, $Pr_{8.33}W_6O_{30}Cl$ and $Nd_{8.33}W_6O_{30}Cl$, was synthesized as single crystals via a high-temperature flux growth method. The reduction of Ce(IV) to Ce(III) was performed in the synthesis of $Ce_{8.64}W_{5.74}O_{30}Cl$ using Zn metal as the reducing agent. All four compounds crystallize in the tetragonal space group $P4_2/nmc$ with a highly disordered and rather unusual arrangement of Ln(III) and W(VI) cations. The three-dimensional crystal structure consists of a complex network of Ln cations occupying multiple coordination environments, including LnO_8 cubes. The level of complexity the disorder adds to the overall structure was considered using calculations for the total information content of the crystal. The temperature dependence of the magnetic susceptibility of $Pr_{8.33}W_6O_{30}Cl$ and $Nd_{8.33}W_6O_{30}Cl$ was measured, and both compounds exhibit paramagnetic behavior across the entire 2 – 300 K temperature range measured.

Keywords: Crystal growth, Cerium(III), Complexity

1. Introduction

Mixed anion compounds that contain both oxygen and at least one other type of anion are of significant interest due to the emergence of such materials as potential IR nonlinear optical materials,[1] photocatalysts,[2] and chloride ion battery components.[3] Differences in ionic radii, valence state, and electronegativity between the different anions can lead to a synergistic effect, resulting in properties that are not observed in compounds containing one type of anion; finally, oxychlorides are relatively uncommon mixed anion compounds.

One rationalization for the limited number of oxychlorides in the literature is the complication of stabilizing mixed anion compounds under typical oxygen rich reaction conditions. While some oxychloride compounds have been synthesized in open systems, the use of redox neutral sealed systems is one viable synthetic method for obtaining these compounds. This approach of using the well-known high temperature flux growth method within sealed silica tubes has proven effective in discovering new reduced oxide and oxyhalide-type compounds.[4–10] Specifically, alkali/alkaline-earth metal chloride melts within a sealed system have proven to be effective in solubilizing a wide variety of starting materials and crystallizing diverse oxide and oxychloride compounds.

A limited number of lanthanide tungsten oxychlorides are known, including $LnWO_4Cl$ (Ln = La – Sm)[11] and $Ln_3WO_6Cl_3$ (Ln = La – Sm, Eu, Gd),[12] which contain W(VI) cations in trigonal bipyramidal and trigonal prismatic coordination environments, respectively. These compounds were initially synthesized as polycrystalline powders combining LaOCl and WO_3 in stoichiometric amounts. Crystals were able to be grown out of a LiCl flux. Both systems have been recently revisited, and it was found these compounds can be targeted by combining the respective lanthanide sesquioxide with the trichloride and WO_3, where excess trichloride can act as fluxing agents in solid-state syntheses.[13, 14] This present work demonstrates the feasibility of preparing lanthanide tungsten oxychlorides by dissolution of all oxide precursors in a pure chloride melt. During attempts to synthesize reduced tungstate compounds, a series of lanthanide tungsten oxychlorides of the compositions $La_{8.64}W_6O_{30.45}Cl$, $Ce_{8.64}W_{5.74}O_{30}Cl$, $Pr_{8.33}W_6O_{30}Cl$ and $Nd_{8.33}W_6O_{30}Cl$, was grown out of a eutectic chloride melt.

An intriguing aspect of this work is the observation of the crystallization of complex structures exhibiting severe anion and cation disorder, a situation that is unlike the expected "perfect" crystallographic order we typically observe in inorganic crystalline structures. The size difference between the oxygen and chloride anions is significant, 1.38 vs 1.81 Å, and can lead to

disorder and structural distortions in cation polyhedra containing both species. In fact, the degree of disorder can be quite substantial and lead to structures that are difficult to describe in the absence of detailing the disorder, as cations can be found to occupy multiple crystallographic locations in more than one type of coordination environment, as well as more than one crystallographic location in the same coordination polyhedron (albeit not simultaneously). Such disorder, however, permits the stabilization of structures and compositions that are unable to achieve a single structural ground state and that are otherwise unable to readily fit the mixed anion coordination environment around the cations. An interesting question to consider is what the maximum degree of disorder can be that nonetheless results in a "crystalline" structure. In this paper, a series of structures are described that exhibit severe disorder, yet form as nicely faceted single crystals. Herein, we report the synthesis of this new series of lanthanide tungsten oxychlorides exhibiting extreme cation and anion disorder and report on their structure and physical properties.

2. Experimental

2.1. Reagents

WO_3 (99.8%, Alfa Aesar) and Zn metal (99.9%, -140 + 325 mesh, Alfa Aesar) were used as received. La_2O_3 (99.9%, Alfa Aesar), CeO_2 (99.99%, Alfa Aesar), and Nd_2O_3 (99.9%, Alfa Aesar) were activated in air at 1000 °C for 12 h and stored in a vacuum desiccator. Pr_6O_{11} (99.99%, Alfa Aesar) was reduced to Pr_2O_3 under 5% hydrogen for 24 h at 1000 °C in a tube furnace. NaCl (Certified A.C.S., Fisher) and CsCl (99%, Alfa Aesar) were dried and stored in an oven at 260 °C.

2.2. Synthesis

Single crystals of $La_{8.64}W_6O_{30.45}Cl$, $Ce_{8.64}W_{5.74}O_{30}Cl$, and $Ln_{8.33}W_6O_{30}Cl$ (Ln = Pr, Nd) were grown out of a molten NaCl/CsCl eutectic flux mixture. For the synthesis of $La_{8.64}W_6O_{30.45}Cl$, a combination of 1 mmol of La_2O_3, 2 mmol WO_3, 1 mmol Zn, and 2 g of a NaCl/CsCl eutectic flux was placed inside a fused silica tube. Table 1 gives the relative ratios of starting reagents and resulting products for the synthesis of each compound. In all cases, the tubes were sealed under vacuum using an oxygen/methane torch. The sealed tubes were placed in a programmable box furnace and heated to 1000 °C at a rate of 10 °C/min, held there for 24 h, cooled to 450 °C at a rate of 6 °C/h, and then returned to room temperature by turning off the furnace. Following the

reaction, the chloride flux was dissolved in water, aided by sonication, and the crystals were isolated via vacuum filtration. Reactions to prepare $La_{8.64}W_6O_{30.45}Cl$ yielded a single-phase product, however, reactions to prepare the Pr and Nd analogs formed alongside Pr_2WO_6 and Nd_2WO_6, respectively. Nonetheless phase pure samples of the Pr and Nd analogs could be obtained by handpicking the desired crystals. Reactions to prepare the Ce analog always resulted in pale yellow crystals of $NaCe(WO_4)_2$ intergrown with $Ce_{8.64}W_{5.74}O_{30}Cl$, making it impossible to isolate a pure sample of the cerium phase.

Table 1
Respective ratios of reagents and flux in the synthesis of each compound and resulting product

Reagents (mmol)	Zn (mmol)	NaCl/CsCl flux	Product	Color
WO_3 : La_2O_3 2 : 1	1.0	2.0 g	$La_{8.64}W_6O_{30.45}Cl$	Black
WO_3 : CeO_2 1 : 1			$Ce_{8.64}W_{5.74}O_{30}Cl$ / $NaCe(WO_4)_2$	Black
WO_3 : Pr_2O_3 1 : 0.5			$Pr_{8.33}W_6O_{30}Cl$ / Pr_2WO_6	Green
WO_3 : Nd_2O_3 1.5 : 0.5			$Nd_{8.33}W_6O_{30}Cl$ / Nd_2WO_6	Black

2.3. Single-Crystal X-ray Diffraction (SXRD)

Single-crystal X-ray diffraction data were collected at 300(2) K on a Bruker D8 QUEST diffractometer equipped with an Incoatec IμS 3.0 microfocus radiation source (MoKα, $\lambda = 0.71073$ Å) and a PHOTON II area detector. The crystals were mounted on a microloop using immersion oil. The raw data reduction and absorption corrections were performed using SAINT and SADABS programs.[15] Initial structure solutions were obtained with SHELXS-2017 using direct methods and Olex2 GUI.[16] Full-matrix least-square refinements against F_2 were performed with SHELXL software.[17] All the structures were checked for missing symmetry with the Addsym program implemented into PLATON software and no higher symmetry was found.[18] The crystallographic data and results of the diffraction experiments are summarized in Table 2.

The structures of all four compounds suffer from a severe disorder of the metal and oxygen sites. An attempt to refine the structures with fully occupied positions results in a model with a high R factor and large satellite residual density peaks. The disorder was modeled by introducing

split sites on the satellite peaks and constraining the total occupancy of the split site to unity using a free variable. After multiple refinement cycles, the occupancies were fixed and a final model was refined. In $Ce_{8.64}W_{5.74}O_{30}Cl$, due to the presence of a large negative electron density peak on the W2A and W2B sites, their occupancies were freely refined, resulting in occupancies of 0.7924 and 0.0804 for W2A and W2B sites, respectively.

2.4. Powder X-ray Diffraction (PXRD)

Powder X-ray diffraction data were collected on a Bruker D2 Phaser powder X-ray diffractometer using Cu Kα radiation. The step scan covered the angular range 5-65° 2θ in steps of 0.04°. The experimental and calculated PXRD patterns were found to be in good agreement (see supporting information Fig. S1-S3).

2.5. Energy-Dispersive Spectroscopy (EDS)

Elemental analysis was performed on single crystals using a TESCAN Vega-3 SBU SEM with EDS capabilities. The crystals were mounted on carbon tape and analyzed using a 20 kV accelerating voltage and an accumulation time of 1 min. As a qualitative measure, EDS confirmed the presence of W, O, Cl, and the respective Ln element of each compound. The absence of extraneous elements, such as the zinc reducing agent, silicon from the reaction vessel, and cesium/sodium cations from the flux mixture, was confirmed within the detection limits of the instrument.

2.6. Magnetic Susceptibility

Magnetic property measurements were performed using a Quantum Design MPMS 3 SQUID magnetometer. Zero-field-cooled (ZFC) magnetic susceptibility measurements were performed from 2 to 300 K in an applied field of 0.1 T. The raw data were corrected for radial offset and sample shape effects according to the method described in the literature.[19]

Table 2
Crystallographic Data for $La_{8.64}W_6O_{30.45}Cl$, $Ce_{8.64}W_{5.74}O_{30}Cl$, and $Ln_{8.33}W_6O_{30}Cl$ (Ln = Pr, Nd)

Chemical formula	$La_{8.64(2)}W_6O_{30.45(8)}Cl$	$Ce_{8.64(2)}W_{5.74(4)}O_{30}Cl$	$Pr_{8.33(2)}W_6O_{30}Cl$	$Nd_{8.33(2)}W_6O_{30}Cl$

Formula weight	2826.01	2782.31	2792.33	2820.07
Crystal system	Tetragonal			
Space group, Z	$P4_2/nmc$, 2			
a /Å	10.0028(3)	9.9519(3)	9.9498(2)	9.9220(2)
c /Å	12.6806(4)	12.5641(3)	12.4348(3)	12.3728(3)
V /Å$_3$	1268.77(9)	1244.35(8)	1231.03(6)	1218.05(6)
ρ_{calcd} /g/cm$_3$	7.397	7.426	7.533	7.689
Radiation (λ, Å)	MoK$_\alpha$ (0.71073)			
μ /mm^{-1}	41.477	42.088	44.252	45.818
T /K	300(2)	301(2)	300(2)	300(2)
Crystal dim. /mm$_3$	0.06×0.04×0.03	0.05×0.04×0.02	0.06×0.02×0.01	0.06×0.02×0.01
2θ range /deg.	2.593 – 29.994	2.611 – 29.997	2.622 – 36.353	2.631 – 29.997
Reflections collected	88375	89428	28743	18857
Data/parameters/restraints	1023/82/0	1003/69/0	1637/77/0	983/78/0
R_{int}	0.0384	0.0362	0.0467	0.0357
Goodness of fit	1.180	1.163	1.103	1.208
R$_1$(I > 2σ(I))	0.0183	0.0266	0.0156	0.0213
wR$_2$ (all data)	0.0437	0.0803	0.0315	0.0508

3. Results and Discussion

3.1. Synthesis

Crystals of $La_{8.64}W_6O_{30.45}Cl$, $Ce_{8.64}W_{5.74}O_{30}Cl$, and $Ln_{8.33}W_6O_{30}Cl$ (Ln = Pr, Nd) were grown out of a eutectic alkali metal chloride flux. Fig. 1 shows a scanning electron microscopy (SEM) image and an optical image of selected single crystals. Chloride melts are known to be suitable solvents for crystal growth of transition metal oxides and have proven useful for crystal growth in similar systems before.[20, 21] In this work a NaCl/CsCl flux was used because of its low eutectic point (486 °C), which allows for a long liquid range for crystal growth. Crystals of $La_{8.64}W_6O_{30.45}Cl$ were initially discovered using a eutectic NaCl/$BaCl_2$ flux, however, the synthesis was eventually optimized by employing a NaCl/CsCl eutectic flux, avoiding the formation of side products containing barium and tungsten. Syntheses of $Pr_{8.33}W_6O_{30}Cl$ and

$Nd_{8.33}W_6O_{30}Cl$ yielded bright green and pink transparent crystals of Pr_2WO_6 and Nd_2WO_6 as byproducts. The desired crystals were visually easily distinguished and manually picked for physical property measurement.

The objective of this work was to obtain lanthanide containing oxides with reduced tungsten cations. To achieve this, Zn metal was introduced to the reactions as a reducing agent, and evacuated silica tubes were used as reaction containers to avoid air re-oxidation. Despite the highly reducing conditions, the compositions obtained from single crystal X-ray diffraction indicate fully oxidized tungsten in all four compounds. The tungsten site deficiency in $Ce_{8.64}W_{5.74}O_{30}Cl$, (see structure description section for details), is charge balanced by the presence of mixed valent Ce^{III}/Ce^{IV} cations. Further evidence for the presence of reduced Ce in $Ce_{8.64}W_{5.74}O_{30}Cl$ is supported by the observed impurity of $NaCe(WO_4)_2$, which contains Ce^{III} cations. The formation of $NaCe(WO_4)_2$, which was found to be intergrown with the target phase, made it impossible to separate the two phases for property measurements.

A large bandgap in fully oxidized tungsten compounds, which are lacking d electrons, is consistent with their lack of color, sodium tungstate being a simple and good example. However, when even a small fraction of tungsten in a compound is reduced to a lower oxidation state, the partial occupation of 5*d* orbitals leads to intense deep blue/black color of such systems. As indicated by the dark color of the studied crystals, tungsten appears to be in fact slightly reduced, although the associated change in stoichiometry is not enough to be detected in the single crystal X-ray diffraction data. To investigate the role of zinc in the formation of the title compounds, a reaction with La was performed without the addition of Zn. It resulted in colorless crystals of $La_2W_2O_9$ and no evidence of $La_{8.64}W_6O_{30.45}Cl$, supporting the presumption that the dark color of the studied crystals stems from partial tungsten reduction by Zn.

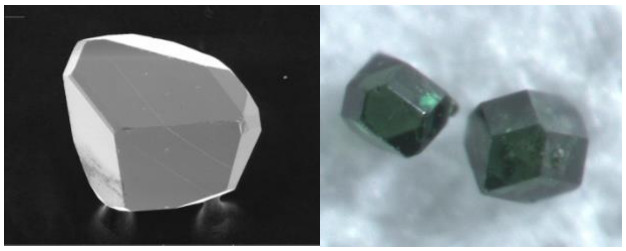

Figure 1. (Left) SEM image of $La_{8.64}W_6O_{30.45}Cl$ and (Right) optical image of $Pr_{8.33}W_6O_{30}Cl$ crystals.

3.2. Crystal Structure Description

The title compounds $La_{8.64}W_6O_{30.45}Cl$, $Ce_{8.64}W_{5.74}O_{30}Cl$, and $Ln_{8.33}W_6O_{30}Cl$ (Ln = Pr, Nd) crystallize in the tetragonal space group $P4_2/nmc$ and represent a new series of oxychloride-type compounds. The structure of these compounds contains a complex arrangement of lanthanide and tungsten atoms, closely related to La_3NbWO_{10}, which was found to be a superstructure of the fluorite structure.[22] These materials differ by the addition of the chloride anion and by severe site disorder found at crystallographic positions of tungsten, oxygen, and the respective lanthanide element. The four compounds are listed as having three unique compositions, which result from slight differences in site occupancies. For this reason, the structure of $La_{8.64}W_6O_{30.45}Cl$ will be described in detail and is depicted in Fig. 2. The other compositions are isostructural and only differ due to slight differences in site occupancies. The crystal structure consists of a framework that is built up of lanthanum in three different coordination environments, LaO_8Cl polyhedra with oxygen disorder, LaO_{12} polyhedra severely disordered with La and O atoms, and regular LaO_8 cubes. The extensive connectivity of the La polyhedra is shown in Fig. 3. Tungsten is found as WO_6 octahedra with slight oxygen disorder and disordered WO_6/WO_7 polyhedra. In this crystal structure description, the idealized structure is discussed, and the disorder is fully described in the supporting information section.

La1 forms a nine coordinate LaO_8Cl coordination polyhedra in the shape of a distorted monocapped tetragonal antiprism with oxygen disorder, shown in Fig. 4, with La-O distances ranging from 2.541(4) Å to 2.955(4) Å and a La-Cl distance of 3.1509(3) Å. La2 is disordered over two positions, La2A and La2B with C_s and C_1 site-symmetries, so that there are three close positions, each of them occupied by La atoms with 24.5 and 33.2% occupancies. The La2 atoms form, depending on the disordered oxygen sites, as either a LaO_{11} or LaO_{12} irregular polyhedron, as shown in Fig. 4, with La-O distances ranging from 2.417(5) Å to 2.828(7) Å. A fully occupied La3 site with D_{2d} symmetry is located in a regular 8-coordinate cube polyhedron (Fig. 4), with uniform bond lengths of 2.501(4) Å.

The W1 site is fully occupied and has an octahedral environment of disordered oxygen atoms (Fig. 4), with W–O distances ranging from 1.83(4) Å to 2.0012(17) Å. W2 atoms are disordered over two C_{2v} symmetry positions, W2A and W2B, in a 0.777(10:0.223(10) ratio. Due to oxygen disorder, the two sites have different coordination environments and form a distorted octahedron

and distorted trigonal prism for W2A and W2B, respectively. There are two additional weak contacts between W2B and O4 atoms with a significantly longer interatomic distance of 2.153(9) Å. A comparison of the strength of these two contacts and the other five bonds can be made using Voronoi tessellation.[23] The Voronoi polyhedron of W2 atom (Fig. 5) exhibits 5 major faces and two small faces, which correspond to the five bonds and the two contacts, respectively. The area of each of the major faces exceeds 16% of the total Voronoi polyhedron area, whereas the two small faces contribute 5.15% each to the total area. Such a value serves as an indication that the two contacts occupy an intermediate state between bonding and nonvalent interactions and, although this cannot be considered as a valent bond, the interaction plays an important role in the W2B site coordination. The W1 sites share corners with W2 and themselves (Fig. 6), forming perpendicular chains running along the *a* and *b* axes, which are then connected through the La sites into a framework.

Considering the chemical composition of $La_{8.64}W_6O_{30.45}Cl$ the oxidation state of W is +6, as supported by charge balance and bond valence sums.[24] Bond valence sum calculations for W were calculated and found to be 6.01, 6.04, and 5.96 for W1, W2A, and W2B, respectively. The partial in situ reduction of Ce(IV) to Ce(III) in $Ce_{8.64}W_{5.74}O_{30}Cl$ is suggested by charge balance and BVS calculations yielding 3.31 when assuming Ce(III) for site Ce3, in addition to the observed impurity containing Ce(III).

The degree of disorder in all of the compositions, $La_{8.64}W_6O_{30.45}Cl$, $Ce_{8.64}W_{5.74}O_{30}Cl$, $Pr_{8.33}W_6O_{30}Cl$ and $Nd_{8.33}W_6O_{30}Cl$, is not unprecedented and a number of structures are known to exhibit similar disorder. For example, $Ce_{18}W_{10}O_{57}$, also exhibits significant disorder, specifically with respect to the tungsten positions, which are disordered over several crystallographic sites, [6] while $Cs_2Mn_3U_6O_{22}$, a layered structure, exhibits partial site occupancies as the crystallographic sites cannot all be simultaneously occupied for size reasons.[25] Clearly, such cation order is not unusual however, in these cases it was much less severe than the cation and anion disorder observed in the title compounds.

In order to understand and quantify the level of complexity the disorder adds to the overall crystal structure of these compounds, calculations for the total information content of the crystal structures were performed in ToposPro[26], as described by Krivovichev.[27] The total information content of a crystal structure, $I_{G,total}$ (bits/unit-cell), provides a quantitative tool for comparing inorganic compounds and helps elucidate what is truly meant when using “complex” to describe a

crystal structure. The total information content of the crystal structure was calculated for $La_{8.64}W_6O_{30.45}Cl$ containing all of the observed site disorder and repeated for an idealized model of the structure with the disorder removed from the lanthanum, tungsten, and oxygen positions. For the disordered model, $I_{G,total}$ = 538.1 bits/unit-cell compared to an $I_{G,total}$ = 308.2 bits/unit-cell for the idealized model. The results of Krivovichev's study of over one hundred thousand crystal structures in the Inorganic Crystal Structure Database (ICSD) places the disordered $La_{8.64}W_6O_{30.45}Cl$ structure into the 'complex' category and the idealized model into the 'intermediate' category, in terms of complexity. A ratio can be considered to compare the two models, $I_{G,total}$ (disordered) : $I_{G,total}$ (idealized) = 1.75 which shows the introduction of site disorder almost doubles the complexity of the structure, which, in turn, appears to be necessary for its stability.

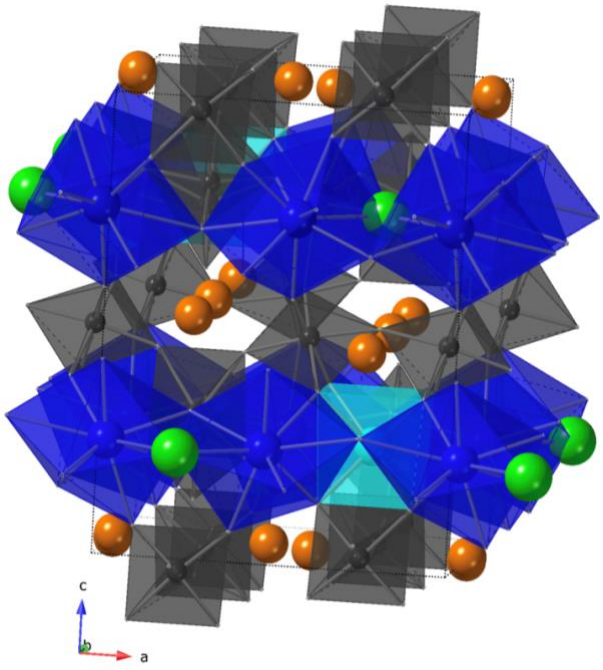

Figure 2. $La_{8.64}W_6O_{30.45}Cl$ viewed down the *b* axis. La1, La2A, La3, W, and Cl are shown in blue, orange, cyan, grey, and green, respectively. Oxygen atoms, La2B, and select La – O and W – O bonds are omitted for clarity.

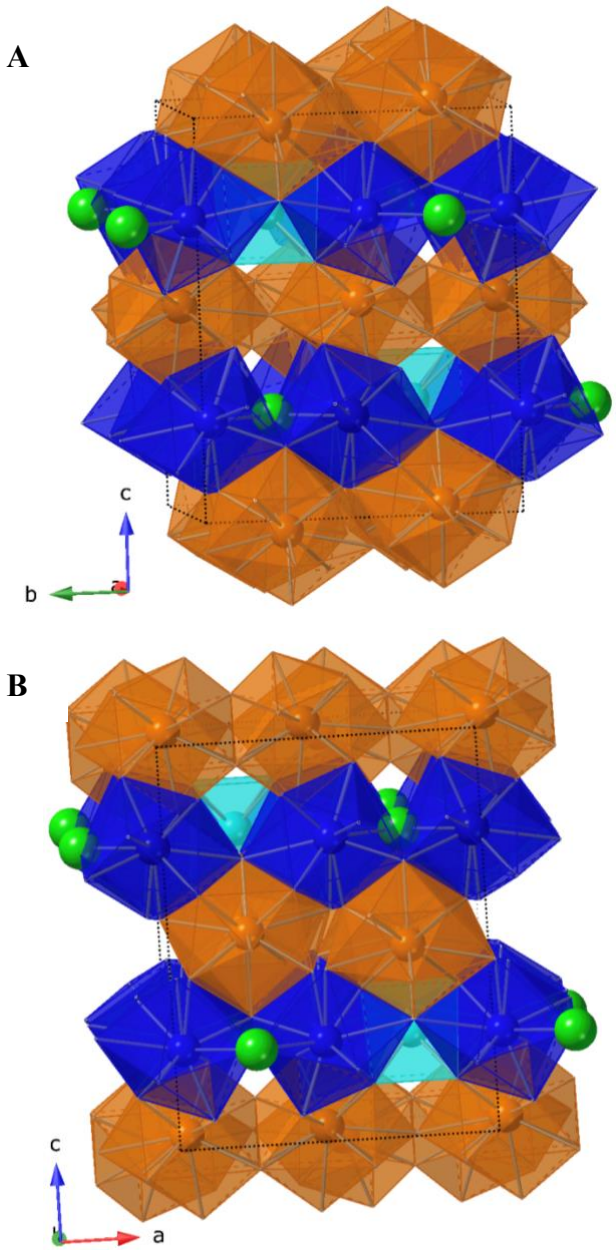

Figure 3. Polyhedral representation of the lanthanum cation network in $La_{8.64}W_6O_{30.45}Cl$ down the (A) *a* and (B) *b* axes. La1, La2, La3, and Cl are shown in blue, orange, cyan, and green, respectively. Oxygen atoms, La2B, and select La-O bonds are omitted for clarity.

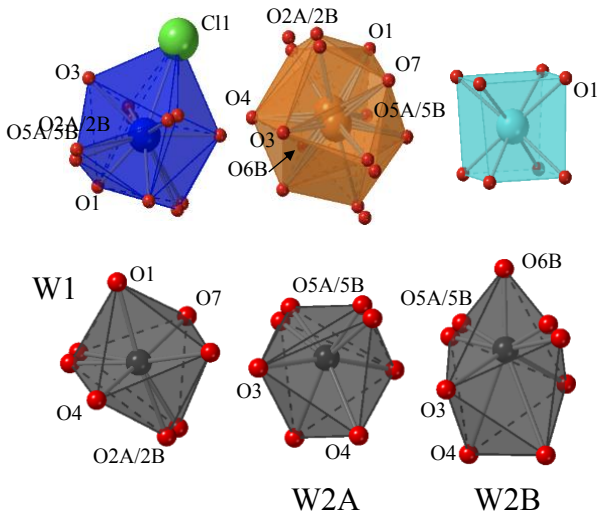

Figure 4. Coordination polyhedra of La1, La2A/2B, La3, W1, W2A, and W2B. La1, La2, La3, W, O, and Cl are shown in blue, orange, cyan, grey, red, and green, respectively. Symmetry equivalent oxygen atoms are not labeled.

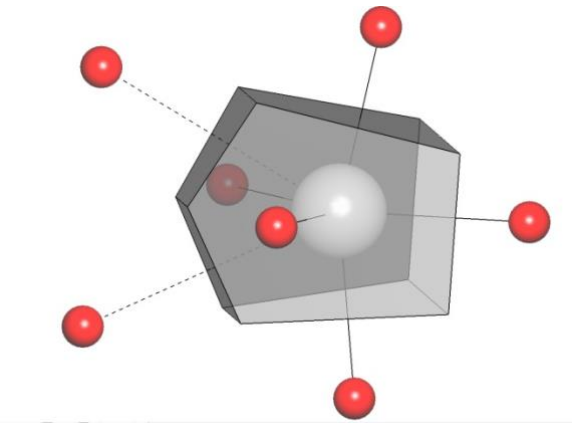

Figure 5. Voronoi polyhedron showing the contribution of the five bonds and two contact points to the total area of site W2.

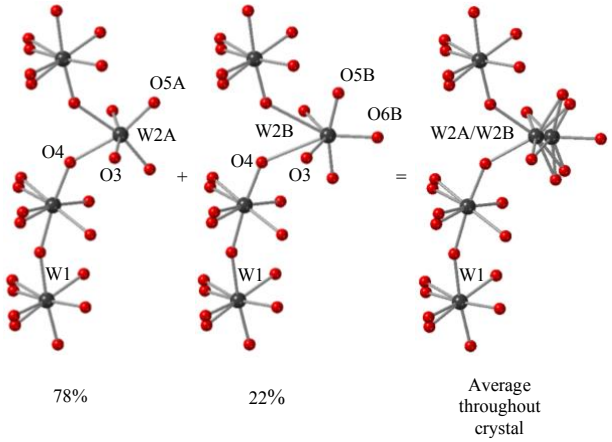

Figure 6. Disordered chains of corner sharing W1 and W2A/W2B atoms and occupancies of W(2A)O_6 octahedra versus W(2B)O_7 polyhedra, located along the *a* axis and perpendicularly along the *b* axis.

3.3. Magnetic Susceptibility

The temperature dependences of the magnetic susceptibilities of $Pr_{8.33}W_6O_{30}Cl$ and $Nd_{8.33}W_6O_{30}Cl$ were measured in an applied field of 0.1 T and are shown in Fig. 7. Considering charge balance in the crystal, the sole magnetic contribution was expected to come from the Ln(III) cations of Pr and Nd, which have 2 and 3 *f* electrons, respectively. Ignoring any contribution from the W(VI) atoms to the magnetism, leaves only the potential interactions between Ln(III) cations due to the extensive connectivity of their polyhedra throughout the structure. However, no differences are observed between zero-field cooled (zfc) and field-cooled (fc) data, and the data reflects paramagnetic behavior down to 2 K with the sole magnetic contribution from non-interacting Pr(III) and Nd(III) cations. The inverse susceptibility data were plotted at high temperatures (200-300 K) and follow the Curie-Weiss law. Effective magnetic moments of $Pr_{8.33}W_6O_{30}Cl$ and $Nd_{8.33}W_6O_{30}Cl$ are in good agreement with the expected values and are listed in Table 3. While no magnetic transition is detected down to 2 K, $Pr_{8.33}W_6O_{30}Cl$ does exhibit a negative Weiss constant, suggesting the presence of antiferromagnetic interactions between Pr(III) cations. The inverse susceptibility data of $Nd_{8.33}W_6O_{30}Cl$ is non-linear, but intersects at essentially 0,0.

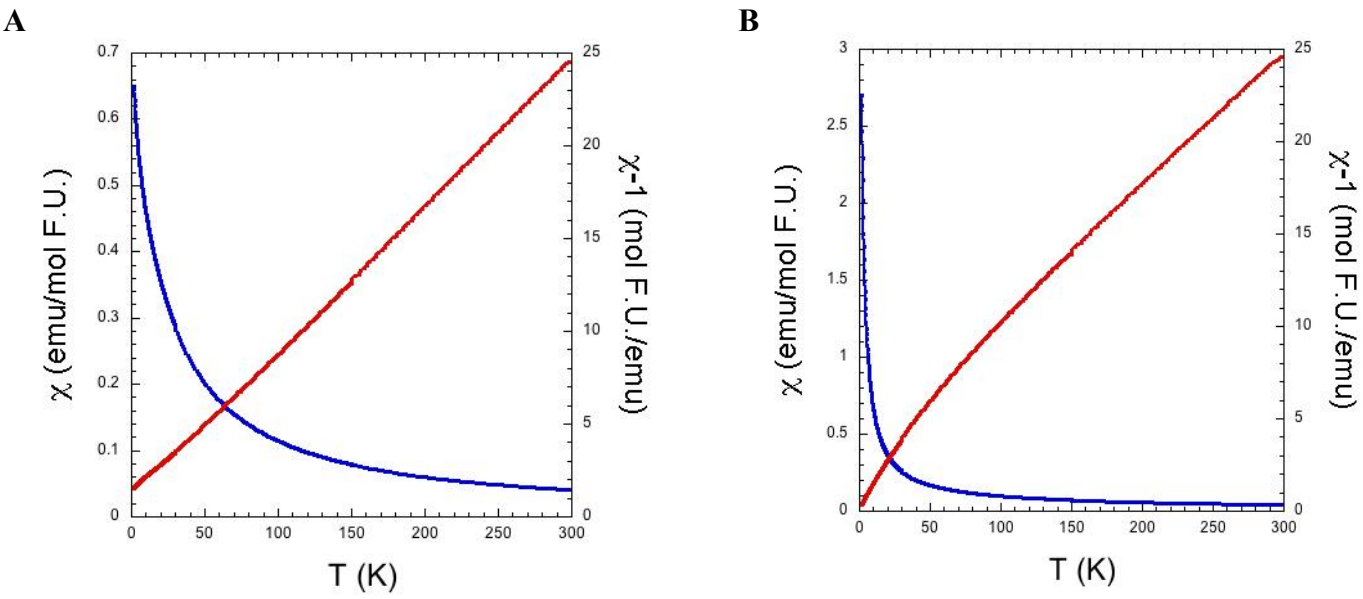

Figure 7. Magnetic susceptibility plot for (A) $Pr_{8.33}W_6O_{30}Cl$ and (B) $Nd_{8.33}W_6O_{30}Cl$ under an applied field of 0.1 T. χ and $1/\chi$ are shown in blue and red, respectively.

Table 3

Observed magnetic moments (μ_{eff}) and calculated moments (μ_{calc}); μ_{calc} were determined assuming that tungsten in present only in the 6+ oxidation state.

Compound	μ_{eff} (μ_B/F.U.) from C-W fit (200 – 300 K)	μ_{calc} (μ_B/F.U.)
$Pr_{8.33}W_6O_{30}Cl$	3.47	3.58
$Nd_{8.33}W_6O_{30}Cl$	3.69	3.62

4. Conclusion

Single crystals of four lanthanum tungsten oxychlorides, $La_{8.64}W_6O_{30.45}Cl$, $Ce_{8.64}W_{5.74}O_{30}Cl$, and $Ln_{8.33}W_6O_{30}Cl$ (Ln = Pr, Nd), were successfully synthesized from oxide starting reagents in a pure chloride melt. The partial reduction of Ce(IV) to Ce(III) in the cerium compound was achieved by adding Zn metal as a reducing agent to the reaction mixture. All compounds consist of a highly disordered arrangement of Ln(III) and W(VI) cations. The magnetic susceptibilities of

$Pr_{8.33}W_6O_{30}Cl$ and $Nd_{8.33}W_6O_{30}Cl$ were measured and display paramagnetic behavior. The extreme amounts of site disorder observed in these compounds classifies them as 'complex' crystal structures within the ICSD, in terms of their total information content.

Acknowledgments

Financial support for this work was provided by the National Science Foundation under DMR-1806279 and is gratefully acknowledged.

Supporting information

PXRD patterns and full description of structure disorder. CCDC 1940692-1940695 contains the supporting crystallographic data for this paper.

References

(1) Zhang, H.; Zhang, H.; Pan, S.; Dong, X.; Yang, Z.; Hou, X.; Wang, Z.; Chang, K. B., Poeppelmeier, K. R., $Pb_{17}O_8Cl_{18}$: A Promising IR Nonlinear Optical Material with Large Laser Damage Threshold Synthesized in an Open System. *J. Am. Chem. Soc.* **2015**, 137, 8360-8363.

(2) Li, J.; Yu, Y., Zhang, L., Bismuth oxyhalide nanomaterials: layered structures meet photocatalysts. *Nanoscale* **2014**, 6, 8473-8488.

(3) Zhao, X.; Zhao-Karger, Z.; Wang, D., Fichtner, M., Metal oxychlorides as Cathode Materials for Chloride Ion Batteries. *Angew. Chem. Int. Ed.* **2013**, 52, 13621-13624.

(4) Bugaris, D. E., zur Loye, H.-C., Materials Discovery by Flux Crystal Growth: Quaternary and Higher Order Oxides. *Angew. Chem. Int. Ed.* **2012**, 51, 3780-3811.

(5) Abeysinghe, D.; Smith, M. D., zur Loye, H.-C., A fresnoite-structure-related mixed valent titanium(III/IV) chlorosilicate, $Ba_3Ti_2Si_4O_{14}Cl$: A flux crystal growth route to Ti(III) containing oxides. *J. Solid State Chem.* **2017**, 250, 128-133.

(6) Abeysinghe, D.; Smith, M. D.; Yeon, J.; Tran, T. T.; Sena, R. P.; Hadermann, J.; Halasyamani, P. S., zur Loye, H.-C., Crystal Growth and Structure Analysis of $Ce_{18}W_{10}O_{57}$: A Complex Oxide Containing Tungsten in an Unusual Trigonal Prismatic Coordination Environment. *Inorg. Chem.* **2017**, 56, 2566-2575.

(7) Cortese, A. J.; Wilkins, B.; Smith, M. D.; Morrison, G., zur Loye, H.-C., Single crystal growth and characterization of the first reduced lanthanum molybdenum oxychloride, $La_{20}Mo_{12}O_{63}Cl_4$, with an unusual trigonal prismatic MoO_6 unit. *Solid State Sci.* **2015**, 48, 133-140.

(8) Read, C. M.; Yeon, J.; Smith, M. D., zur Loye, H.-C., Crystal growth, structural characterization, cation-cation interaction classification, and optical properties of uranium(VI) containing oxychlorides, $A_4U_5O_{16}Cl_2$ (A = K, Rb), $Cs_5U_7O_{22}Cl_3$, and AUO_3Cl (A = Rb, Cs). *CrystEngComm* **2014**, 16, 7259-7267.

(9) Abeysinghe, D.; Gerke, B.; Morrison, G.; Hsieh, C. H.; Smith, M. D.; Pottgen, R.; Makris, T. M., zur Loye, H.-C., Synthesis, characterization, and properties of reduced europium molybdates and tungstates. *J. Solid State Chem.* **2015**, 229, 173-180.

(10) Abeysinghe, D.; Smith, M. D.; Yeon, J.; Morrison, G., zur Loye, H.-C., New Lanthanide Mixed-Valent Vanadium(III/IV) Oxosilicates, $Ln_4V_{5-x}Zn_xSi_4O_{22}$ (Ln = La, Ce, Pr, and Nd), Crystallizing in a Quasi Two-Dimensional Rutile-Based Structure. *Inorg. Chem.* **2016**, 55, 1821-1830.

(11) Brixner, L. H.; Chen, H. Y., Foris, C. M., Structure and luminescence of the orthorhombic *Ln*WO_4Cl-type rare earth halo tungstates. *J. Solid State Chem.* **1982**, 45, 80-87.

(12) Brixner, L. H.; Chen, H. Y., Foris, C. M., Structure and luminescence of some rare earth halotungstates of the type $Ln_3WO_6Cl_3$. *J. Solid State Chem.* **1982**, 44, 99-107.

(13) Dorn, K. V.; Blaschkowski, B.; Forg, K.; Netzsch, P.; Hoppe, H. A., Hartenbach, I., Prism Inside: Spectroscopic and Magnetic Properties of the Lanthanide(III) Chloride Oxidotungstates(VI) $Ln_3Cl_3[WO_6]$ (*Ln* = La - Nd, Sm - Tb). *Z. Anorg. Allg. Chem.* **2017**, 643, 1642-1648.

(14) Schustereit, T.; Schleid, T.; Hoppe, H. A.; Kazmierczak, K., Hartenbach, I., Chloride derivatives of lanthanoid(III) *ortho*-oxidotungstates(VI) with the formula *Ln*$Cl[WO_4]$ (*Ln* = Gd-Lu): Synthesis, crystal structures and spectroscopic properties. *J. Solid State Chem.* **2015**, 226, 299-306.

(15) Krause, L.; Herbst-Irmer, R.; Sheldrick, G. M., Stalke, D., Comparison of Silver and Molybdenum Microfocus X-Ray sources for Single-Crystal Structure Determination. *J. Appl. Crystallogr.* **2015**, 48, 3-10.
(16) Dolomanov, O. V.; Bourhis, L. J.; Gildea, R. J.; Howard, J. A. K., Puschmann, H., OLEX2: A Complete Structure Solution, Refinement and Analysis Program. *J. Appl. Crystallogr.* **2009**, 42, 339-341.
(17) Sheldrick, G. M., Crystal Structure Refinement with SHELXL. *Acta Crystallogr., Sect. C: Struct. Chem.* **2015**, 71, 3-8.
(18) Speck, A., Structure Validation in Chemical Crystallography. *Acta Crystallogr., Sect. D: Biol. Crystallogr.* **2009**, 65, 148-155.
(19) Morrison, G., zur Loye, H.-C., Simple correction for the sample shape and radial offset effects on SQUID magnetometers: Magnetic measurements on Ln_2O_3 (Ln = Gd, Dy, Er) standards. *J. Solid State Chem.* **2015**, 221, 334-337.
(20) Juillerat, C. A.; Klepov, V. V.; Morrison, G.; Pace, K. A., zur Loye, H.-C., Flux crystal growth: a versatile technique to reveal the crystal chemistry of complex uranium oxides. *Dalton Trans.* **2019**, 48, 3162-3181.
(21) Liu, X.; Fechler, N., Antonietti, M., Salt melt synthesis of ceramics, semiconductors, and carbon nanostructures. *Chem. Soc. Rev.* **2013**, 42, 8237-8265.
(22) Vu, T. D.; Barre, M.; Adil, K.; Jouanneaux, A.; Suard, E., Goutenoire, F., Investigation of the La_2O_3-Nb_2O_5-WO_3 ternary phase diagram: Isolation and crystal structure determination of the original La_3NbWO_{10} material. *J. Solid State Chem.* **2015**, 229, 129-134.
(23) Blatov, V. A.; Shevchenko, A. P., Serezhkin, V. N., Crystal Space Analysis by means of Voronoi-Dirichlet Polyhedra. *Acta Crystallogr.* **1995**, A51, 909-916.
(24) Brese, N. E., O'Keeffe, M. O., Bond-Valence Parameters for Solids. *Acta Crystallogr.* **1991**, B47, 192-197.
(25) Read, C. M.; Gordon, E. E.; Smith, M. D.; Yeon, J.; Morrison, G.; Whangbo, M.-H., zur Loye, H.-C., Synthesis of the Layered Quaternary Uranium-Containing Oxide $Cs_2Mn_3U_6O_{22}$ and Characterization of its Magnetic Properties. *Inorg. Chem.* **2015**, 54, 5495-5503.
(26) Blatov, V. A.; Shevchenko, A. P., Proserpio, D. M., Applied Topological Analysis of Crystal Structures with the Program Package ToposPro. *Cryst. Growth Des.* **2014**, 14, 3576-3586.
(27) Krivovichev, S. V., Which Inorganic Structures are the Most Complex? *Angew. Chem. Int. Ed.* **2014**, 53, 654-661.

For Table of Contents Only

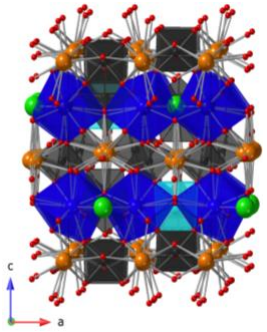

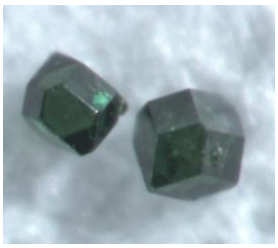

The compositions $La_{8.64}W_6O_{30.45}Cl$, $Ce_{8.64}W_{5.74}O_{30}Cl$, $Pr_{8.33}W_6O_{30}Cl$ and $Nd_{8.33}W_6O_{30}Cl$ were grown as single crystals via a high temperature flux growth method. These compounds exhibit extreme cation and anion disorder which is necessary for the stability of the complex structure. The dark color of the materials suggests partial tungsten reduction, with the addition of Zn to the reactions being imperative for their formation. Magnetic susceptibility measurements of $Pr_{8.33}W_6O_{30}Cl$ and $Nd_{8.33}W_6O_{30}Cl$ show paramagnetic behavior down to 2 K.